Spectrochimica Acta Part A 75 (2010) 825–829

Contents lists available at ScienceDirect

Spectrochimica Acta Part A: Molecular and Biomolecular Spectroscopy

journal homepage: www.elsevier.com/locate/saa

Synthesis, characterization and luminescence properties of Eu(III) and Tb(III) complexes with novel pyrazole derivatives and 1,10-phenanthroline

Fei-Long Hu, Xian-Hong Yin*, Yan Mi, Shan-Shan Zhang, Wei-Qiang Luo

College of Chemistry and Ecological Engineering, Guangxi University for Nationalities, Nanning 530006, PR China

ARTICLE INFO

Article history:
Received 30 April 2009
Received in revised form
25 November 2009
Accepted 1 December 2009

Keywords:
Lanthanide
Fluorescence property
Pyrazole

ABSTRACT

Two novel pyrazole-derived ligands, 3-chloro-6-(3,5-dimethyl-1H-pyrazol-1-yl)picolinic acid (CDPA) and 3-chloro-6-(3,5-dimethyl-1H-pyrazol-1-yl)-N-phenylpicolinamide (CDPP) were prepared by 3,6-dichloropicolinic acid (DCPA). Their complexes with terbium(III) and europium(III) were synthesized. The complexes were characterized by elemental analysis, infrared spectra, ^{1}H NMR and TG–DTG. Furthermore, the above complexes using 1,10-phenanthroline as a secondary ligand were also synthesized and characterized. The luminescence properties of these complexes in solid state were investigated. The results suggested that Tb(III) complexes exhibit more efficient luminescence than Eu(III) complexes and the fluorescence of the complexes with 1,10-phenanthroline as a secondary ligand was prominently stronger than that of complexes without this ligand., and the three ligand (DCPA), (CDPP) and (CDPA) are excellent sensitizers to Eu(III) and Tb(III) ion.

© 2009 Elsevier B.V. All rights reserved.

1. Introduction

Fluorescent compounds have attracted much attention recently due to their potential applications. When they are fluorescent in the solid state, they may be good candidates for photoluminescent or electroluminescent materials [1–3]; when they are fluorescent in solution, they can be used as fluorescent sensor molecules for research in biology or environmental science [4,5]. In the development of new luminescent materials, organic electroluminescence (OEL) has been studied extensively for its applications because of its low drive voltage, suitability for integrated circuit and potential application for large flat panel display [6,7]. As some lanthanide ions, e.g. Eu^{3+} and Tb^{3+} possess good luminescence characteristics based on the transitions between the 4f energy levels, a series of compounds activated Eu^{3+} and Tb^{3+} have been studied for practical application as phosphors and laser materials [8].

The investigations into the relationship between the structures or organic ligands and the energy levels of lanthanide ions will give evidences for designing high luminescent lanthanide organic complexes. In this work, two novel pyrazole-derived ligands named 3-chloro-6-(3,5-dimethyl-1H-pyrazol-1-yl)-N-phenylpicolinamide and 3-chloro-6-(3,5-dimethyl-1H-pyrazol-1-yl)picolinic acid and their Eu(III) and Tb(III) complexes were synthesized. Both of the two novel pyrazole ligands have rigid conjugated planar structure [9], the carboxylate group or carboxyl group, which would be of potential applications in time-resolved fluoroimmunoassay and DNA probe. In addition, we prepared Eu(III) and Tb(III) pyrazole complexes using 1,10-phenanthroline as a secondary ligand since it is widely used as assistant antenna groups for photosensitising lanthanide ion. The luminescence properties of all these complexes in solid state were investigated in detail. The synthetic route of ligands are listed in Scheme 1.

2. Experimental

2.1. Materials

3,6-Dichloropicolinic acid and other reagents were purchased and used as without further purification. Rare earth chlorides were prepared according to the literature [10].

2.2. Methods

Contents of carbon, hydrogen and nitrogen were determined using an Elementar vario ELanalyzer. Content of Tb(III) was determined by EDTA titration. Infrared spectra (4000–400 cm^{-1}) were recorded with samples as KBr discussing a Nicolet NEXUS 670 FTIR spectrophotometer. ^{1}H NMR spectra was measured by using a Varian Mercury-300 nuclear magnetic resonance spectrometer with DMSO as solvents and TMS as internal reference. Fluorescence measurements were made on a Hitich F-4500 spectrometer. All the pH measurements were made with a pHS-3 digital pH-meter (Shanghai REX instrument factory, Shanghai, China) with

---

* Corresponding author. Tel.: +86 771 3064863; fax: +86 771 3260896.
E-mail address: yxhphd@163.com (X.-H. Yin).

1386-1425/$ – see front matter © 2009 Elsevier B.V. All rights reserved.
doi:10.1016/j.saa.2009.12.006

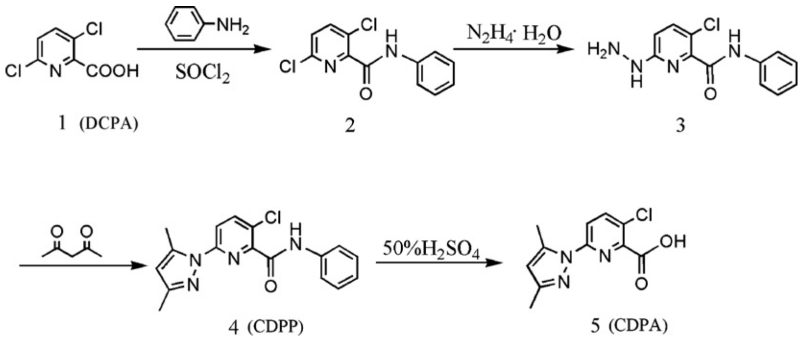

Scheme 1.

a combined glass-calomel electrode. Thermogravimetric (TG) and differential thermal gravimetry (DTG) were performed in the nitrogen atmosphere using a Shimadzu DTG 40 system at a heating rate of 10 °C min^{-1} from 30 °C to 800 °C.

2.3. Synthesis of the ligand

2.3.1. Synthesis of 3,6-dichloro-N-phenylpicolinamide (2)

To a solution of 3,6-dichloropicolinic acid (DCPA) (9.55 g, 0.05 mol) in anhydrous $CHCl_3$ (150 mL), sulfuryl dichloride (50 mL) was added dropwise under nitrogen atmosphere at 0 °C with continuous stirring for 3 h. Excess solvent was removed under reduced pressure and the residue was cooled to 0 °C with ice bath. Aniline (5.11 g 0.055 mol) added dropwise, triethylamine in acetonitrile (100 mL) was added to the residue. The solution was stirred for another 1 h. The solvent was removed and the crude product was purified by recrystallization from ethanol to give the flaxen solid 2 (12.5 g) after drying in vacuum. Yield: 90%; mp 130–132 °C. IR(KBr), ν_{max} (cm^{-1}): 3350 (N–H), 1690 (C=O) 1600, 1525, 1490, 1340 (skeleton of Ph, Py), 1255 (C–N), ^{1}H NMR(DMSO-d$_6$, ppm), δ: 8.02 (d, 1H, Py), 7.84 (d, 1H, Py), 7.27–7.53 (m, 5H, C_6H_5), 9.80 (s 1H, NH). Elemental analytical (calc.) C% 53.86 (53.96); H% 3.08 (3.02), N% 10.39 (10.49).

2.3.2. Synthesis of 3-chloro-6-(3,5-dimethyl-1H-pyrazol-1-yl)-N-phenylpicolinamide (3)

Hydrazine hydrate (50 ml, 85%) was added to a solution of 2 (5 g) in toluene under stirring at 110 °C for 1 h, then cooled to room temperature and ice water (100 ml) was added to the mixture, a white precipitate formed. The precipitate was collected by filtration and washed with water. Recrystallization from ethanol give the compound 3 (2.45 g). Yield: 50%; mp 140–142 °C. IR(KBr), ν_{max} (cm^{-1}): 3300 (N–H), 1690 (C=O), 1520 (C=N), 1500 (C=C). ^{1}H NMR(DMSO-d$_6$, ppm), δ: 7.8 (d, 1H, Py), 7.74 (d, 1H, Py), 7.15–7.41 (m, 5H, C_6H_5), 9.55 (s 1H, NH). Elemental analytical (calc.) C% 62.96 (62.48); H% 4.68 (4.63), N% 17.39 (17.15).

2.3.3. Synthesis of 3-chloro-6-(3,5-dimethyl-1H-pyrazol-1-yl)-N-phenylpicolinamide (4)

Pentane-2,4-dione (0.91 g 9.1 mmol) was added to solution of 3 (2 g 7.6 mmol) in toluene under stirring and this mixture was heated at 120 °C for 1.5 h. Excess solvent was removed under reduced pressure and 50 ml ice water was added to the mixture, a white precipitate formed. The precipitate was collected by filtration and washed with water. Recrystallization from ethanol (2.5 g). Yield: 80%: mp 221–223 °C. IR(KBr), ν_{max} (cm^{-1}): 3300 (N–H), 1650 (C=O), 1610, 1575, 1530, 1450, 1340 (skeleton of Ph, Py and Pyraz), 1250 (C–N), ^{1}H NMR(DMSO-d$_6$, ppm), δ: 8.05 (d, 1H, Py), 7.91 (d, 1H, Py), 7.28–7.55 (m, 5H, C6H5), 6.08 (s, 1H, Pyraz), 9.84 (s 1H, NH), 2.30–2.55 (s, 6H, CH_3). Elemental analytical (calc.) C% 62.42 (62.48); H% 4.68 (4.63); N% 17.10 (17.15).

2.3.4. Synthesis of 3-chloro-6-(3,5-dimethyl-1H-pyrazol-1-yl)picolinic acid (5)

Compound (CDPP) (2 g 6.1 mmol) was added to a solution of sulfuric acid (10.0 ml 50%) under stirring at room temperature for 10 min, and the mixture was heated to 130 °C incubated for 3.5 h, then was cooled to room temperature and sodium bicarbonate was added until the pH value was 1, a white precipitate formed, The precipitate was collected by filtration. Recrystallization from ethanol give the ligand 3-chloro-6-(3,5-dimethyl-1H-pyrazol-1-yl)picolinic acid (CDPA) (1.15 g). Yield 80%; mp 180–82 °C, IR(KBr), ν_{max} (cm^{-1}): 3400 (OH), 1713 (C=O), 1582 (C=N), 1572, 1560, 1469, 1382 (skeleton of ph, Py and Pyraz), 1256 (C–N), ^{1}H NMR(DMSO-d$_6$, ppm), δ 11.05 (s, 1H, OH), 8.15 (d, 1H, Py), 7.94 (d, 1H, Py), 6.16 (s, 1H, Pyraz), 2.21–2.58 (m, 6H, CH_3).

2.4. Synthesis of the complexes

The complex $Eu(DCPA)_3{\cdot}3H_2O$ was prepared according the following steps. A solution of DCPA (0.286 g, 1.5 mmol) in ethanol (10 ml) was added dropwise to a solution of $EuCl_3{\cdot}6H_2O$ (0.148 g, 0.5 mmol) in ethanol (10 ml) under stirring and this mixture was heated at 60 °C for 24 h. Then the pH value of the mixture was adjusted to 6 by adding an aqueous solution of sodium hydroxide, pale yellow precipitate obtained was separated by filtration, washed three times with ethanol and dried in vacuum for 48 h. The yield was about 60% based on the amount of $EuCl_3$ used.

The complex $Eu(DCPA)_2(Phen){\cdot}H_2O$ was prepared as follows: 1,10-phenanthroline (0.095 g, 0.5 mmol) in ethanol (10 ml) was added to a solution prepared as described for $Eu(DCPA)_3{\cdot}3H_2O$ above. The mixture was heated under stirring at 80 °C for 24 h. Then the pH value of the mixture was adjusted to 6 by adding an aqueous solution of sodium hydroxide. The pale yellow precipitate obtained was filtered, washed three times with ethanol and dried in vacuum for 48 h, yield: 75%. Similarly, the other complexes $Eu(CDPP)_3{\cdot}2H_2O$, $Eu(CDPP)_2(Phen){\cdot}3H_2O$, $Eu(CDPA)_3{\cdot}4H_2O$, $Eu(CDPA)_2(Phen){\cdot}3H_2O$, $Tb(DCPA)_3{\cdot}4H_2O$, $Tb(DCPA)_2(Phen)$, $Tb(CDPP)_3{\cdot}3H_2O$, $Tb(CDPA)_3{\cdot}4H_2O$, $Tb(CDPP)_2(Phen){\cdot}3H_2O$ and $Tb(CDPA)_2(Phen)\ {\cdot}3H_2O$ were prepaered.

All complexes are soluble in DMF, DMSO and methanol, a little soluble in ethanol, ethyl acetate and acetone, insoluble in benzene, diethyl ether and THF.

3. Result and discussion

3.1. Properties of the complexes

Analytical data for the complexes were presented in Table 1. The results of elemental analysis indicated that the composition

Table 1
Elemental analytical data for the complexes.

Complex	M (%) found (calc.)	C (%) found (calc.)	H (%) found (calc.)	N (%) found (calc.)
$Eu(DCPA)_3 \cdot 3H_2O$	19.50 (19.51)	27.76 (27.75)	1.53 (1.55)	5.39 (5.39)
$Eu(DCPA)_2(Phen) \cdot H_2O$	20.78 (20.76)	39.56 (39.37)	1.96 (1.93)	7.68 (7.65)
$Eu(CDPP)_3 \cdot 2H_2O$	13.06 (13.03)	52.76 (52.52)	4.09 (4.06)	14.38 (14.41)
$Eu(CDPP)_2$ $(Phen) \cdot H_2O$	15.12 (15.15)	55.18 (55.10)	3.96 (3.92)	13.99 (13.97)
$Eu(CDPA)_3 \cdot 4H_2O$	15.56 (15.54)	40.23 (40.53)	3.88 (3.81)	12.86 (12.89)
$Eu(CDPA)_2(Phen) \cdot 2H_2O$	17.42 (17.46)	46.93 (46.91)	3.56 (3.59)	12.89 (12.87)
$Tb(DCPA)_3 \cdot 4H_2O$	19.73 (19.77)	26.43 (26.89)	1.56 (1.76)	5.28 (5.23)
$Tb(DCPA)_2(Phen)$	22.155 (22.04)	39.20 (39.97)	1.23 (1.68)	7.75 (7.77)
$Tb(CDPP)_3 \cdot 3H_2O$	13.34 (13.34)	51.42 (51.42)	4.13 (4.15)	14.12 (14.11)
$Tb(CDPP)_2$ $(Phen) \cdot 3H_2O$	15.23 (15.20)	52.83 (52.83)	4.15 (4.14)	13.37 (13.39)
$Tb(CDPA)_3 \cdot 4H_2O$	16.01 (16.13)	40.51 (40.24)	3.66 (3.79)	12.95 (12.80)
$Tb(CDPA)_2(Phen) \cdot 3H_2O$	17.65 (17.75)	45.61 (45.60)	3.70 (3.71)	12.50 (12.51)

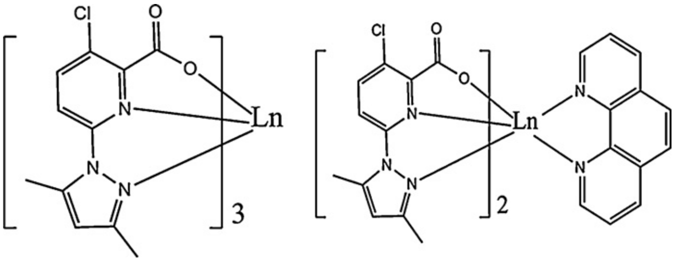

Fig. 1. Chemical structural formula of the complexes.

of the complexes conforms to $Eu(DCPA)_3 \cdot 3H_2O$, $Eu(CDPP)_3 \cdot 2H_2O$, $Eu(DCPA)_2(Phen) \cdot H_2O$, $Eu(CDPP)_2(Phen) \cdot 3H_2O$, $Eu(CDPA)_3 \cdot 4H_2O$, $Eu(CDPA)_2(Phen) \cdot 3H_2O$, $Tb(DCPA)_3 \cdot 4H_2O$, $Tb(DCPA)_2(Phen)$, $Tb(CDPP)_3 \cdot 3H_2O$, $Tb(CDPA)_3 \cdot 4H_2O$ $Tb(CDPP)_2(Phen) \cdot 3H_2O$, and $Tb(CDPA)_2(Phen) \cdot 3H_2O$. All the complexes were found to be soluble in H_2O, DMSO, DMF, slightly soluble in ethanol.

On the basis of above evidence and analyses, the possible structural formula of the complexes is shown in Fig. 1.

3.2. *IR spectra*

The IR spectral data of the ligands and their lanthanide(III) complexes were listed in Table 2. In the ligands of DCPA and CDPA, broad weak bands at 3445 and 3440 cm^{-1} were observed, which can be attributed to the CO–OH. In addition, high intensity sharp bands are observed at 1713 cm^{-1} in DCPA and 1730 cm^{-1} in CDPA which are attributed to the C=O group. The high intensity bands at 1601 cm^{-1} (DCPA), 1603 cm^{-1} (CDPP), 1606 cm^{-1} (CDPA) were assigned to C=C. These bands confirm the presence of the aromatic rings. Medium intensity bands in the 1578–1469 cm^{-1} region were regarded as a combination of C=N of the pyridine or pyrazole ring and aromatic C=C stretching vibrations.

Table 2
Characteristic IR bands (cm^{-1}) of the ligands and their complexes.

Compounds	νO–H	νC=O	νC=N	νC–N	νM–O	νM–N
DCPA	3445	1713	1558	1227		
CDPP		1721	1564	1259		
CDPA	3440	1730	1543	1234		
$Eu(DCPA)_3 \cdot 3H_2O$	3365	1698	1542	1233	421	518
$Eu(DCPA)_2(Phen) \cdot H_2O$	3521	1640	1545	1221	421	496
$Eu(CDPP)_3 \cdot 2H_2O$	33295	1679	1528	1261	413	505
$Eu(CDPP)_2$ $(Phen) \cdot H_2O$	3345	1680	1531	1226	420	509
$Eu(CDPA)_3 \cdot 4H_2O$	3340	1715	1520	1244	412	505
$Eu(CDPA)_2(Phen)$ $\cdot 2H_2O$	3325	1701	1557	1225	419	522
$Tb(DCPA)_3 \cdot 4H_2O$	3501	1695	1538	1230	420	515
$Tb(DCPA)_2(Phen)$	3452	1689	1543	1221	420	500
$Tb(CDPP)_3 \cdot 3H_2O$	3487	1675	1526	1250	415	506
$Tb(CDPP)_2$ $(Phen) \cdot 3H_2O$	3365	1688	1529	1226	418	507
$Tb(CDPA)_3 \cdot 4H_2O$	3438	1647	1603	1247	422	503
$Tb(CDPA)_2(Phen)$ $\cdot 3H_2O$	3385	1706	1545	1225	422	520

In the case of Ln(III) complexes we observed the following changes. All the complexes exhibited broad medium intensity bands at about 3300–3500 cm^{-1}, which were assigned to the coordinated water molecule. The high intensity bands appearing around 1713 cm^{-1} (DCPA), 1721 cm^{-1} (CDPP) and 1730 cm^{-1} (CDPA) which were ascribed to C=O downshifted to 1638–1680 cm^{-1} in Ln(III) complexes, this confirms that the oxygen atoms of RCOO– coordinated to Ln(III) ions successfully. The high intensity bands appearing around 1561 cm^{-1} (DCPA), 1586 cm^{-1} (CDPP) and 1564 cm^{-1} (CDPA) which due to C=N in pyridine or pyrazole ring, downshifted to about 1564 cm^{-1}, 1531 cm^{-1} and 1558 cm^{-1} in these Ln(III) complexes respectively. The obvious shifts indicated that the C=N groups of the ligands coordinated to the Ln(III) ions through nitrogen atoms. The complexes showed medium intensity bands in the region 550–590 cm^{-1} which were assigned to Ln–N [11,12] and 423–435 cm^{-1} assigned to Ln–O modes.

According to the results above, we reached the conclusion that the ligands coordinated to the Ln(III) ions via the oxygen atoms of the carboxyl groups and the nitrogen atoms of the pyridine, pyrazole and 1,10-phenanthroline. The elemental analysis and IR spectra results lead us to propose the general chemical composition.

3.3. *Fluorescence studies*

The fluorescence characteristics of Eu(III) and Tb(III) complexes in solid state were measured at room temperature under PMT voltage 400 V. Under identical experimental conditions, the fluorescence characteristics of all complexes in solid state were shown in Fig. 2. The excitation peak of the europium complexes is from 307 to 360 nm. The emission peaks are 593 and 617 nm which can be attributed to the $^5D_0 \rightarrow {}^7F_{1,}$ $^5D_0 \rightarrow {}^7F_2$ transitions, respectively. It shows that the energy transfer from the ligand to Eu^{3+} take place and exhibits the fluorescent characteristic of Eu^{3+}. In the Eu(III) complexes, we could see that the emission band $^5D_0 \rightarrow {}^7F_2$ is obviously higher than the other emission band $^5D_0 \rightarrow {}^7F_1$ (Fig. 2a, c and e), which suggesting low symmetry around the Eu^{3+} ion in the complexes. Because the forbidden $^5D_0 \rightarrow {}^7F_2$ electric dipole transition is the sensitive to the coordinative environment of Eu^{3+} ion, the asymmetric microenvironment causes the polarization of Eu^{3+} ion under the influence of the electric field of the surrounding ligands, which increase the probability for the electric dipole transition. The excitation peak of the europium complexes is from 307 to 360 nm. The emission peaks are 490, 546, 585 and 622 nm which can be attributed to the $^5D_4 \rightarrow {}^7F_6$, $^5D_4 \rightarrow {}^7F_5$, $^5D_4 \rightarrow {}^7F_4$, and $^5D_4 \rightarrow {}^7F_3$ transitions, respectively. The emission band $^5D_4 \rightarrow {}^7F_5$ is distinctly stronger than the other emission bands $^5D_4 \rightarrow {}^7F_6$, $^5D_4 \rightarrow {}^7F_4$ and $^5D_4 \rightarrow {}^7F_3$ in the Tb(III) complexes [13,14] (Fig. 2b, d and f).

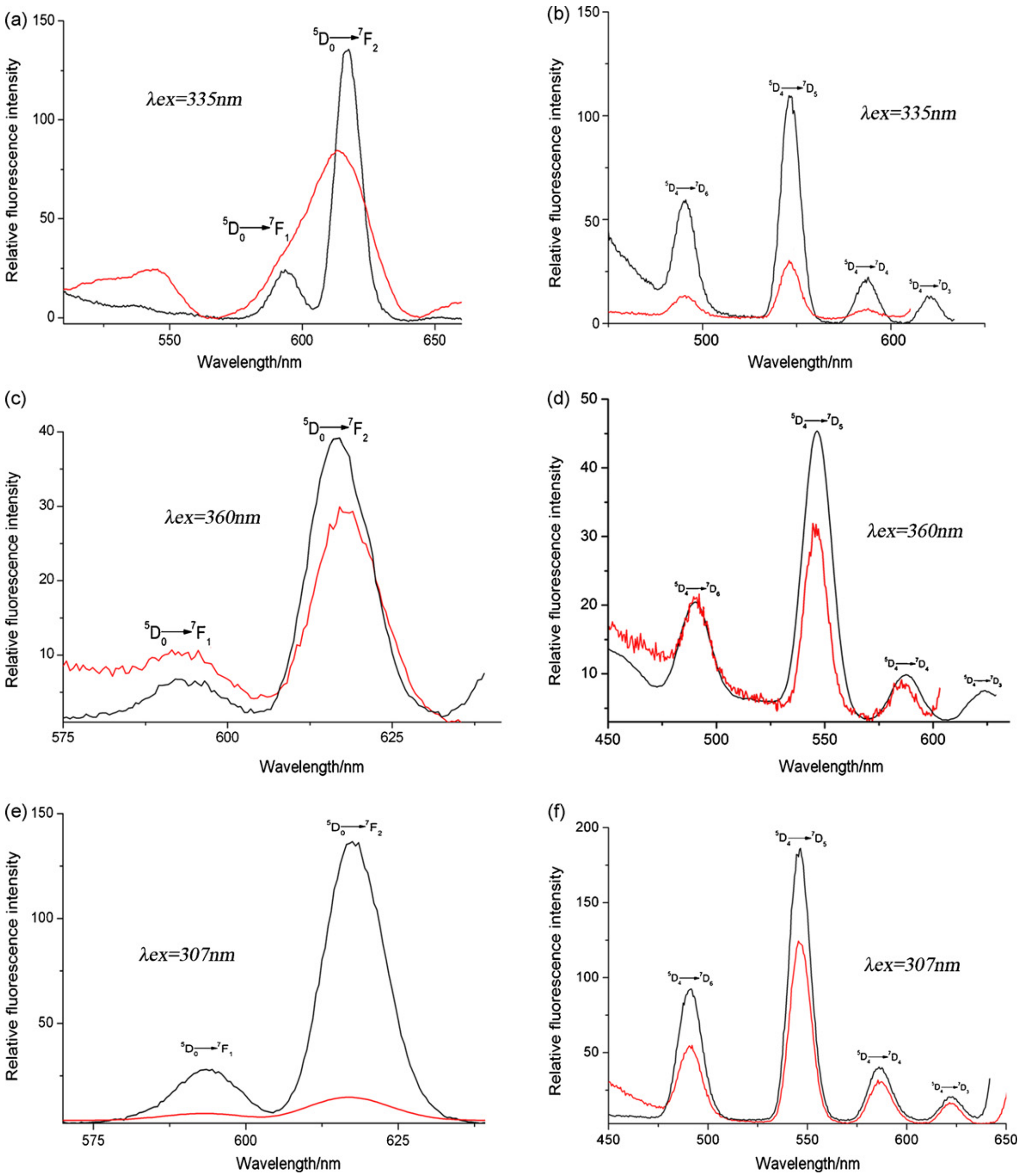

Fig. 2. Subparts (a), (c) and (e) represent the Eu(III) complexes with DCPA, CDPP and CDPA, respectively. Subparts (b), (d) and (f) represent the corresponding Tb(III) complexes. Black line indicate these complexes using 1,10-phenanthroline as a secondary ligand. The excitation and emission slit widths were 5 nm and the PMT voltage was 400 V.

It is shown in Fig. 2 that the complexes show the characteristic emissions of Eu(III) and Tb(III). Among these complexes, it is clearly observed that the fluorescence intensity of Tb(III) complexes are much stronger than that of corresponding Eu(III) complexes. This is mostly because that the luminescence of Ln(III) complexes are related to the efficiency of the intramolecular energy transfer between the triplet level of the ligands and the emitting level of the ions, which depends on the energy gap between the two levels, probable the energy gap between the ligand triplet level and the emitting level of Tb(III) favors to the energy transfer process compared with Eu(III) complexes. To obtain highly efficient luminescence, 1,10-phenanthroline was introduced as a sensitizer. As seen in the spectra, when the phen was introduced into the Eu(III) and Tb(III) complexes, the intensity of the high-energy bands enhanced markedly (Fig. 2). This could be due to the superposition of the $\pi \rightarrow \pi^*$ transiton of phen, implying that the energy transfer from phen to the Eu(III) and Tb(III) ion strongly enhances emission from the phen-doped complexes [15–17]. This data implies that both ligand and phen are binding to the Eu^{3+} and Tb^{3+} ion and that their presence together affords a strong sensitization of the Eu^{3+} and Tb^{3+} emission [18].

It is also observed that the fluorescence intensity of Ln(III) complexes with DCPA or CDPA is about three times as that of Ln(III) complexes with CDPP and these complexes would be considered as promising candidates for applications in organic light-emitting devices, sensory materials and luminescent probes.

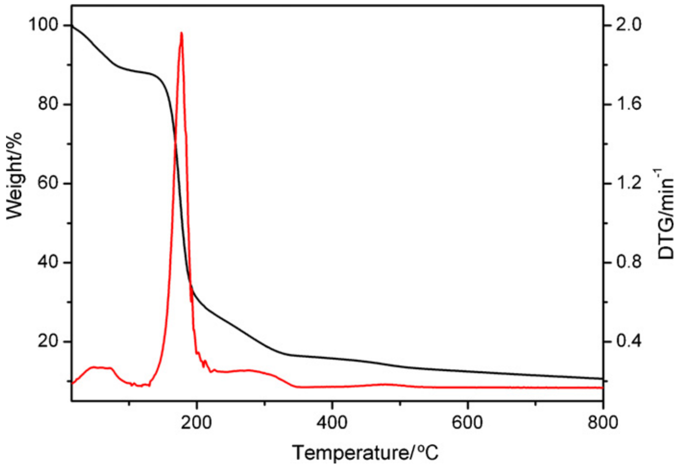

Fig. 3. TG–DTG curves of $Tb(DCPA)_3{\cdot}4H_2O$ under N_2 atmosphere with the heating rate of 10 °C min^{-1}.

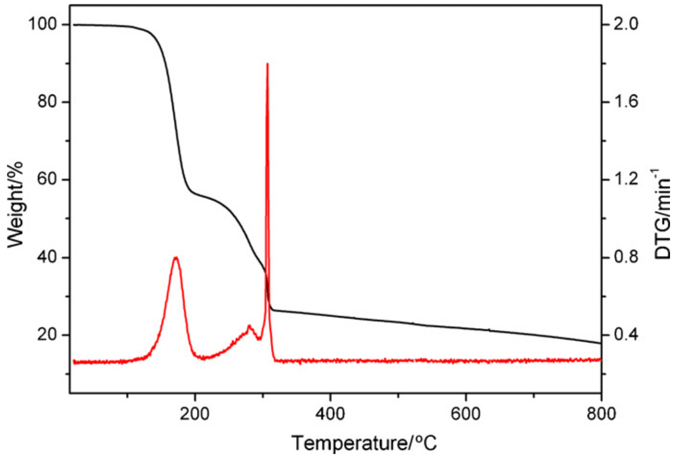

Fig. 4. TG–DTG curves of $Tb(DCPA)_2(phen)$ under N_2 atmosphere with the heating rate of 10 °C min^{-1}.

3.4. *Themogravimetric analysis*

The two complexes $Tb(DCPA)_3{\cdot}3H_2O$ and $Tb(DCPA)_2(Phen)$ were selected to perform thermal decomposition analysis.

Figs. 3 and 4 show the thermogravimetric and differential thermal gravimetry curves obtained by heating $Tb(DCPA)_3{\cdot}4H_2O$ and $Tb(DCPA)_2phen$ in nitrogen atmosphere with the heating rate of 10 °C min^{-1}. The decomposition takes place between 30 °C and 800 °C. In the TG–DTG curves, there are two main successive mass loss stages from 30 °C to 800 °C for the two complexes. The first mass loss satge of $Tb(DCPA)_3{\cdot}3H_2O$ starts at 50 °C, end at 90 °C and reaches the largest rate at 65 °C with mass loss percentage of 10.3%, this stage roughly coincides with the value of 9.0%, calculated for the loss of four water molecules from the complex. Similarly, the first mass loss stage of $Tb(DCPA)_2(phen)$ starts at 140 °C end at 187 °C and reaches the largest rate at 171 °C with mass loss percentage of 44.6%, this stage roughly coincides with the value of 52.9%, calculated for the loss of two DCPA molecules from the complex.

The second stage of $Tb(DCPA)_3{\cdot}4H_2O$ with 68.5% mass loss starts at 150 °C, finishes at 317 °C and reaches the largest rate at 177 °C. The mass loss percentage is near the loss of three DCPA molecules from the complex (calc.71.25%). And the second stage of $Tb(DCPA)_2(phen)$ with 31.1% mass loss start at 187 °C, finishes at 314 °C and reaches the largest rate at 307 °C. The mass loss percentage is near the loss of the phen molecule from the complex (cacl. 25.03%). The residual percentage weight (observed 21.17% for $Tb(DCPA)_3{\cdot}4H_2O$ and 26.6% for $Tb(DCPA)_2(phen)$) at the end of the decomposition of the complex is consistent with the formation of Tb_4O_7.

4. Conclusions

The synthesis and fluorescence properties of Eu(III) and Tb(III) complexes with new pyridine derived ligands, 3,6-dichloropicolinic acid, 3-chloro-6-(3,5-dimethyl-1H-pyrazol-1-yl)picolinic acid, 3-chloro-6-(3,5-dimethyl-1H-pyrazol-1-yl)-N-phenylpicolinamide and 1,10-phenanthroline were reported. Acccording to the IR spectra data, coordination of the ligands to Ln(III) ions was occurring at the oxygen atoms of the carbonyl goups and the nitrogen atoms of the pyridine (pyrazole) ring and 1,10-phenanthroline. The fluorescence data indicate that Tb(III) complexes with these ligands exhibit much highter emission than corresponding Eu(III) complexes. It is worth noting that addition of 1,10-phenanthroline to the Eu(III) and Tb(III) complexes lead to the formation of complexes with over 30% higher fluorescence emission. In addition, Tb(III) complexes with CDPA emit stronger green emission than Tb(III) complexes with corresponding CDPP and DCPA complexes. Based on those results, a series of new pyrazole-derived ligand could be designed and synthesized to optimize the luminescent properties of these lanthanide ions complexes.

Acknowledgements

The authors thank the National Natural Science Foundation of China (20761002), PR China, The Natural Science Foundation of Guangxi (0832080).

References

[1] C.F. Peter, C. Elena, B. James, Chem. Rev. 99 (1999) 3625.
[2] J.Y. Lee, Q.D. Liu, D.R. Bai, Y.J. Kang, Y. Tao, S. Wang, Organometallics 23 (2004) 6205.
[3] X.J. Xu, Y. Liao, G. Yu, H. You, C.A. Di, Z.M. Su, D. Ma, Q. Wang, S.Y. Li, S.Q. Wang, J.P. Ye, Y.Q. Liu, Chem. Mater. 19 (2007) 1740.
[4] S. Banthia, A. Samanta, J. Phys. Chem. B 110 (2006) 6437.
[5] S.J. Toal, K.A. Jones, D. Magde, W.C. Trogler, J. Am. Chem. Soc. 127 (2005) 11661.
[6] R.H. Friend, R.W. Gymer, A.B. Homes, J.H. Buroughes, R.N. Marks, C. Taliani, D.D.C. Bradley, D.A. Dos Santos, J.L. Brédas, M. Lögdlund, W.R. Salaneck, Nature 397 (1999) 121.
[7] P.K.H. Ho, D.S. Thomas, R.H. Friend, N. Tessler, Science 285 (1999) 233.
[8] N. Filipescu, W.F. Sager, F.A. Serafin, J. Phys. Chem. 68 (1964) 3324.
[9] K. Zhao, X.H. Yin, Y. Feng, J. Zhu, C.W. Lin, Acta Crystallogr. E64 (2008) m407.
[10] A.J. Chandrasekhar, Imaging Technol. 16 (1990) 158.
[11] K. Ueno, A.E. Martell, J. Phys. Chem. 60 (1956) 1270.
[12] G. Percy, Spectrochim. Acta 32A (1976) 1287.
[13] S.M. Ying, J.G. Mao, Cryst. Growth Des. 6 (2006) 964.
[14] M.D. Regulacio, M.H. Pablico, J.A. Vasquez, P.N. Myers, S. Gentry, M. Prushan, S. Wah, T. Chang, S.L. Stoll, Inorg. Chem. 47 (2008) 1512.
[15] J.G. Kang, H.G. Cho, J.G. Kim, K.S. Choi, Mater. Chem. Phys. 91 (2005) 172.
[16] J.C. Lee, K.S. Choi, H.K. Cho, J.G. Kang, J. Lumin. 127 (2007) 332.
[17] M.D. McGehee, T.B. Bergstedt, C. Zhang, A.P. Saab, M.B. O'Regan, G.C. Bazan, V.I. Srdanov, A.J. Heeger, Adv. Mater. 11 (1999) 1349.
[18] S.T. Frey, M.L. Gong, W.D. Horrocks Jr., Inorg. Chem. 33 (1994) 3229.